

The study on visible photocatalytic activity of an oxalate-extended Pb(II) coordination polymer

Jia-Jia Zhang^a, Yu-Chang Wang^b, Juan Jin^{a,c,*}, Wen-Fu Yan^c, Ying-Chun Guo^a, Yuan-Peng Wang^a, Pei-Yu Duan^a, Li-Xia Yang^a, Fa-Ju Hou^a, Jun-Shen Liu^{a,*}

^aSchool of Chemistry and Materials Science, Ludong University, Yantai, Shandong 264025, P.R. China, emails: jinjuan8341@163.com (J. Jin), 2639358348@qq.com (J.-J. Zhang), 1413560348@qq.com (Y.-C. Guo), 1925844133@qq.com (Y.-P. Wang), 2719678780@qq.com (P.-Y. Duan), 37154690@qq.com (L.-X. Yang), 275209606@qq.com (F.-J. Hou), liujunshen@163.com (J.-S. Liu)

^bYantai Valiant Fine Chemicals Co., Ltd., Yantai, Shandong 264006, P.R. China, email: yuchang8341@163.com (Y.-C. Wang)

^cCollege of Chemistry and State Key Laboratory of Inorganic Synthesis and Preparative Chemistry, Jilin University, Changchun, Jilin 130023, China, email: yanwf@jlu.edu.cn (W.-F. Yan)

Received 14 November 2022; Accepted 7 April 2023

ABSTRACT

Under the hydrothermal method, a Pb(II) coordination polymer [Pb(ox)(phen)₂]_n·5H₂O 1 (ox = oxalate, phen = 1,10-phenanthroline) was obtained. Ox ligands exhibit a μ₂-coordination mode, which connect Pb²⁺ centers into a 1-D single-chain with ancillary phen molecules. Interestingly, adjacent phen molecules between the chains exist π...π stacking interaction, which extend the 1-D chain into a 2-D supramolecular layer. Compound 1 showed outstanding photocatalytic performance and the degradation efficiency of methylene blue with H₂O₂ could reach 95.69% under the irradiation of visible light at pH = 10. In addition, 5 cycles of degradation experiments were also carried out, and it was found that the degradation efficiency values with and without H₂O₂ were reduced by 1.46% and 1.08%, respectively. It was also discussed that which free radical played the dominant role in the photocatalytic process. What's more, we speculated the possible reaction mechanism based on the Mott-Schottky curve. Meanwhile, the UV visible diffuse reflection of compound 1 was also investigated.

Keywords: Water pollution; Photocatalysis; Visible light; Coordination polymer; Oxalate

1. Introduction

Ecological pollution problems have been more and more severely with the rapid growth of industry. Especially, the pulp and paper industry consumes a large amount of water resources and releases a large amount of organic highly polluted sewage that needs to be treated every year [1]. In order to solve this problem, scientists have studied many methods, such as membrane separation technology [2], adsorption separation technology [3], etc. However, these methods of degrading sewage have some disadvantages. For example, membrane separation technologies tend to form adhesive

layers, which can slow down their treatment of wastewater [4,5]. And adsorption separation method is very important for the selection of adsorbents [6,7]. The emergence of photocatalyst effectively solves the shortcomings of the above methods and becomes a good choice to solve the problem of sewage [8–10]. Photocatalysts such as titanium dioxide and cadmium sulfide have been widely used in sewage treatment. However, these photocatalysts have the disadvantages of narrow spectral response range and low quantum conversion efficiency [8]. Therefore, it is a great challenge to develop a photocatalyst with excellent photocatalytic performance [11,12].

* Corresponding authors.

Coordination polymers have ordered structure with high specific surface area [13] and high tunability [14–16]. Therefore, they have received extensive attention in catalysis, optics, etc [17–21]. Especially, coordination polymers have unique structural properties that increase its photoreactivity by increasing the number of reactive sites [22–27]. So it is a wise decision to use coordination polymers to degrade organic pollutants in sewage. Chen et al. [28] first treated the sewage with coordination polymers as a photocatalysis [22]. Since then, people have paid more and more attention to the application of coordination polymers in photocatalytic degradation of sewage [22,29,30]. However, few examples of polymers degrading sewage under visible light irradiation have been reported. In order to synthesize coordination polymers with good photocatalytic performance under visible light, the choice of organic ligands is also crucial [31]. Oxalic acid (H_2ox) has strong coordination ability and excellent conjugate system [32], so it plays an important role in forming coordination polymers and improving photocatalytic degradation efficiency. Dai et al. [33] found that adding H_2ox into coordination polymer system could improve the degradation efficiency of bisphenol A. Dridi et al. [34] synthesized a three-dimensional compound with oxalate ligands and demonstrated it had a excellent photocatalytic degradation effect on methylene blue. 1,10-phenanthroline (phen) as a bidentate ligand, the N atoms can easily occupy the empty orbital of metal ions [35]. So, it is widely used in the synthesis of coordination polymers [36]. Also, it can improve the efficiency of photocatalytic degradation with good excellent conjugate system. Lu et al. [37] studied four novel coordination polymers based on flexible dicarboxylates and different ligands. They compared their photocatalytic properties and found that coordination polymers containing phen ligands showed superior degradation of methyl violet [37]. The photocatalytic performance of metallic lead is also excellent [38]. Based on the above idea, we selected oxalic acid, 1,10-phen and Pb^{2+} as raw materials to synthesize a Pb(II) coordination polymer $[Pb(ox)(phen)_2] \cdot 5H_2O$ 1 according to Zhu et al. [39]. It is used for the degradation of methylene blue (MB) in water on visible light and the experimental results show that the degradation rate can reach up to 95.69% with the addition of H_2O_2 , which is higher than the degradation rate of some compounds reported [40–43]. This indicates that compound 1 is a potential visible light catalyst.

2. Experimental sections

2.1. Materials and characterization

The raw materials used in this experiment were purchased from commercial channels without further treatment. Elemental analysis was performed on a PerkinElmer 2400 LS II Elemental Analyzer: PerkinElmer Enterprise Management (Shanghai) Co., Ltd., No. 1670, Zhangheng Road, Zhangjiang Hi-Tech Park, Shanghai, China. Infrared (IR) spectra in the 4,000–400 cm^{-1} region was recorded on a PerkinElmer Spectrum One FT-IR Spectrometer, using powder samples on a KBr plate. Thermogravimetric (TG) properties were obtained on a Perkin Elmer TGA 7 instrument heated at 10°C/min in air. The UV-Vis diffuse reflection spectra (DRS) was recorded by SolidSpec-3700 UV-Vis Spectrophotometer in the range of 240–800 nm and baseline correction using

$BaSO_4$. The absorbance of MB solution was measured by 722E type visible spectrophotometer with absorption wavelength of 664 nm, and the photocatalytic degradation efficiency of compound 1 was calculated by the Eq. (1).

$$\frac{(A_t - A_0)}{A_0} \quad (1)$$

A standard three-electrode system was adopted on Chenhua Chi750e electrochemical workstation with Ag/AgCl as the reference electrode, platinum electrode as the opposite electrode and Na_2SO_4 solution (1 mol/L) as the electrolyte.

2.2. Synthesis of compound 1

2.2.1. $[Pb(ox)(phen)_2] \cdot 5H_2O$ 1

A mixture of $Pb(CH_3COO)_2 \cdot 3H_2O$ (0.50 mmol, 163 mg), 1,10-phen (0.50 mmol, 90 mg), H_2ox (0.50 mmol, 63 mg) were dissolved into 15 mL H_2O . The solvent was stirred for 4 h at room temperature. Its pH was then adjusted to 6 with saturated oxalic acid solution. The obtained mixture was sealed in a 25 mL Teflon autoclave reactor and heated at 170°C for 4 d under autogenous pressure. The yellow crystals were finally getting in 48% yield (based on Pb(II)). Anal. Calcd. for $C_{26}H_{18}N_4O_9Pb$ (%): C, 42.85; H, 2.35; N, 7.68. Found: C, 42.24; H, 2.44; N, 7.58. IR (cm^{-1}): 1,609 s, 1,568 s, 1,511 s, 1,428 s, 1,303 s, 1,223 s, 1,139 m, 1,091 m, 845 s, 768 m, 729 s, and 563 s.

2.3. X-ray crystallography

Crystallographic data for compound 1 was collected on a Siemens SMART CCD diffractometer with Mo-K α radiation ($\lambda = 0.71073 \text{ \AA}$). The structure was solved by direct methods using the SHELXTL program and specified on F² using SHELXL-2014 package by full-matrix least-squares methods. All non-hydrogen atoms of compound 1 obey anisotropy and all hydrogen atoms of the ligands were positioned at calculated positions and refined by the riding mode. CCDC number is 2190555. Solvent molecules were treated with squeeze and 5 H_2O molecules were shown for compound 1 by elemental analysis and TG. The crystallographic data of compound 1 is shown in Table 1.

2.4. Photocatalytic degradation

The photocatalytic performance of compound 1 was tested by the degradation rate of methylene blue (MB) under the irradiation of visible light. Prepare a MB solution with an absorbance of 1 and adjust the pH = 4, 7, 10 of MB with NaOH and H_2SO_4 . The 40 mg of compound 1 was dissolved in 80 mL MB solution and dark for 30 min to achieve adsorption and desorption. Finally, the solution was irradiated with a xenon lamp and visible light for 70 min, centrifuged every 10 min and its absorbance was measured.

2.5. Electrochemical testing

The 5 mg compound 1 was dispersed in the mixed solution of 0.5 mL ethanol, 0.5 mL pure water and 5 μ L Nafion, then the mixed solution was vibrated ultrasonic for 30 min. The above suspension was coated on the cleaned

glass carbon electrode (ϕ 3 mm). Finally, the working electrode was prepared by drying at room temperature.

3. Results and discussion

3.1. Hydrothermal synthesis of coordination polymer

The most common method for synthesizing coordination polymers is hydrothermal synthesis. The reaction time, temperature and pH have an extremely important influence on the crystal formation, so we explored the optimal reaction conditions in the trial. Compound 1 was obtained from the reaction for 4 d in a 170°C oven. The crystals shape are regular and have a high purity at pH = 6.

3.2. Structural description

3.2.1. $[Pb(ox)(phen)_2] \cdot 5H_2O$

X-ray single-crystal analysis revealed that compound 1 is an oxalate-bridged chained Pb^{2+} coordination polymer with ancillary phen ligands. It crystallizes in space group C_{mmm} . As shown in Fig. 1, its asymmetric unit contains one Pb(II) atom (PbI), one oxalate ion (ox) and two phen molecules. Pb(II) is located in a five-fold coordinated by four ox oxygen atoms (O1, O1a, O1b, O1c) and one phen nitrogen atom (N1) (Fig. S1). The bond length of Pb–O_{ox} is 2.690(9) Å and that of Pb–N_{phen} is 2.723(10) Å. Both bond lengths are comparable to those in the reported compounds, proving that these bonds are present [44,45]. As shown in Fig. 1, ox ligands adopt the μ_2 -bridging mode, which use four O atoms (O1, O1a, O1d, O1e) bond two Pb(II) centers, expanding the compound 1 into a 1-D limitless chain in a direction with phen

as auxiliary ligands. Interestingly, phen ligands are located on the both sides of the chain, where adjacent phen molecules between the layers form the $\pi \dots \pi$ stacking interactions with the plane-to-plane distance (d) of 3.26 Å, which make the 1-D chain into a 2-D supramolecular layer (Fig. 2).

3.3. IR analysis

The IR spectral analysis of the compound 1 is shown in Fig. S2. The infrared absorption peaks (cm^{-1}) of the compound: 1,609 s, 1,568 s, 1,511 s, 1,428 s, 1,303 s, 1,223 m, 1,139 m, 1,091 m, 845 s, 768 m, 729 s, and 563 s.

The peak at 1,609 cm^{-1} is the stretching vibration of the (COO) of carboxylic acid [31,39], which indicates that the oxalic acid has coordinated with Pb(II). Also, it can be observed that there are obvious peaks at 1,568 and 1,223 cm^{-1} , which are ascribed to the stretching vibration of C=N and C–N, respectively [46], indicating that phen has also been introduced into the resulting framework of compound 1.

3.4. TG analysis

The thermal stability of compound 1 was tested at 25°C–800°C. As shown in Fig. 3, compound 1 undergoes two steps of weight loss. The first step in weight loss should be ascribed to the removal of lattice water molecules (Found:

Table 1
Crystallographic data for compound 1

| | |
|--|------------------------|
| Empirical formula | $C_{26}H_{18}N_4O_9Pb$ |
| M | 737.61 |
| Crystal system | Orthorhombic |
| Space group | C_{mmm} |
| a (Å) | 19.3535(10) |
| b (Å) | 6.8144(4) |
| c (Å) | 9.6731(10) |
| α (°) | 90 |
| β (°) | 90 |
| γ (°) | 90 |
| V (Å ³) | 1,275.71(17) |
| Z | 2 |
| D_c (g/cm ³) | 1.686 |
| μ (Mo-K α) (mm ⁻¹) | 13.177 |
| $F(000)$ | 612 |
| Total data | 1,489 |
| Unique data | 735 |
| R_{int} | 0.0474 |
| GOF | 1.081 |
| R_1 [$I > 2\sigma(I)$] | 0.0448 |
| wR_2 [all data] | 0.1048 |

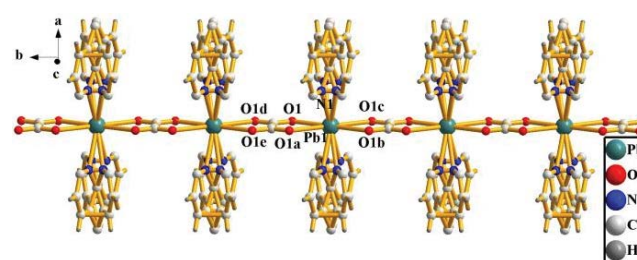


Fig. 1. The 1-D chain structure for compound 1 (symmetric code a: $-x+1, -y+1, -z+1$; b: $x, y, -z+1$; c: $-x+1, -y+1, z$; d: $-x+1, -y+2, z$; e: $-x+1, -y+2, -z+1$).

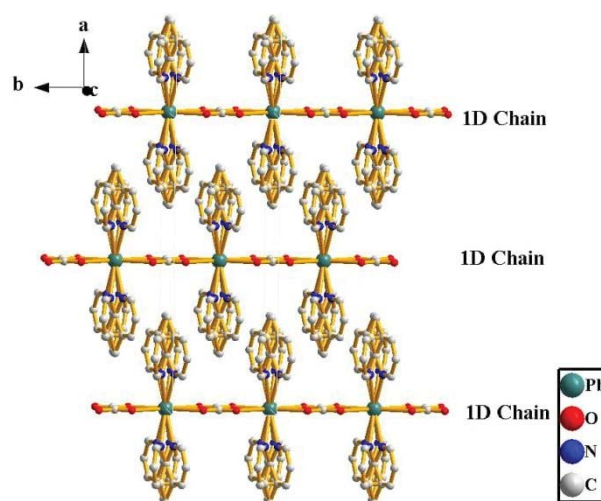


Fig. 2. The 2-D chain structure for compound 1.

10.96%, Calcd.: 12.21%). The weight loss in the second-step is in the temperature range of 250°C–300°C and the weight loss is attributed to the loss of all the ligands (Found: 58.40%, Calcd.: 57.53%). The final material left is PbO (Found: 30.64%, Calcd.: 30.26%).

3.5. UV-Vis absorption spectra and band gap

We studied the UV-Vis diffuse reflection of compound 1 and estimated its band gap value. The UV-Visible diffuse reflection test consequence showed that compound 1 had a photoresponse in the UV region. According to the Tauc plot method [47], we reckoned the band gap energy (E_g) of compound 1 based on the relationship of $(\alpha hv)^2$ and hv and it was 2.58 eV (Fig. 4). After calculation, it can be seen that the compound 1 had a relatively narrow band gap value, which explained that it had a photoresponse at visible light.

The band gap was counted by Eq. (2).

$$(\alpha hv)^{1/n} = A(hv - E_g) \tag{2}$$

where α is absorption index, h is Planck constant, v is frequency, A is constant [22].

3.6. Photocatalytic property

In this experiment, MB was used as a template dye to test the photocatalytic property of compound 1 under the irradiation of visible light with xenon lamps [48]. According to the study, pH and H_2O_2 have important effects on the photocatalytic property of coordination polymer. It was found that the degradation rate of MB was obviously higher with the increase of pH (Fig. 5). The reason may be that with the

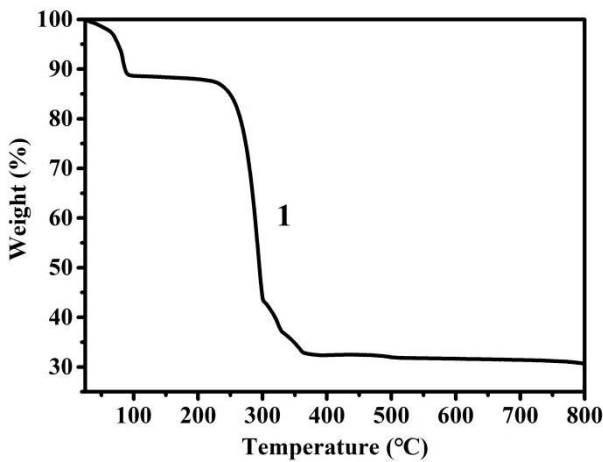


Fig. 3. Thermogravimetric curve of compound 1.

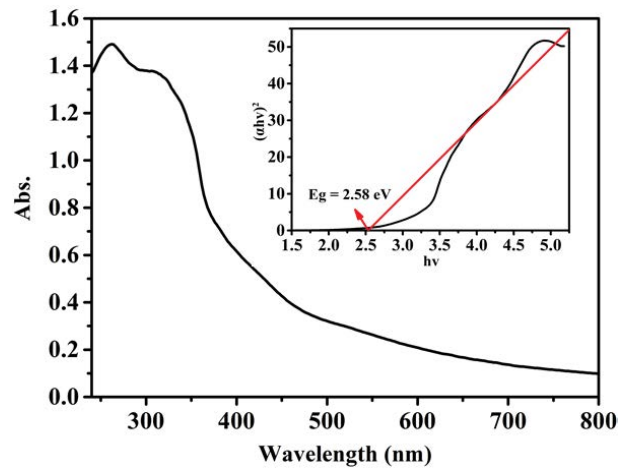


Fig. 4. UV-Vis absorption spectra and Tauc plots of compound 1.

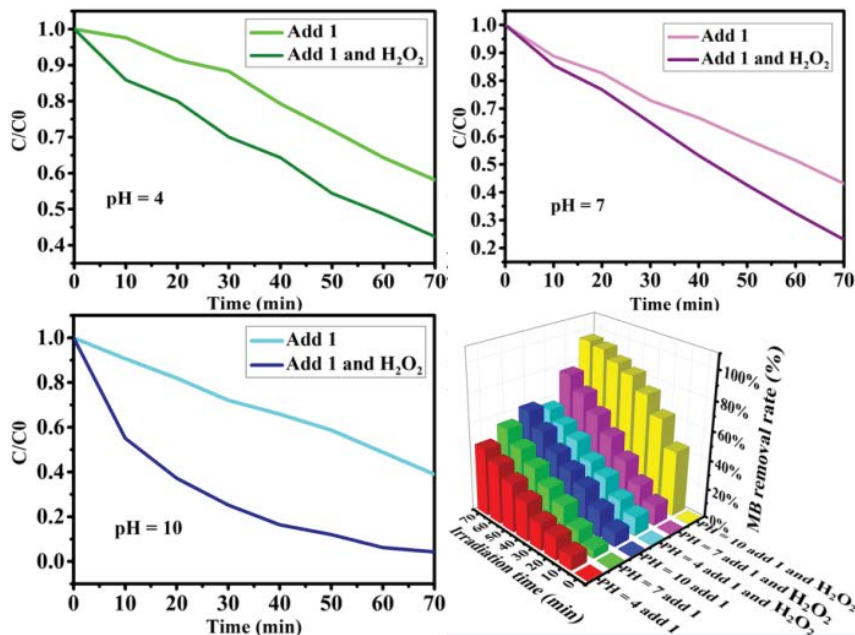


Fig. 5. Methylene blue degradation profile of different conditions under visible light irradiation.

increase of pH, the OH⁻ content in the solution increases, so that more OH⁻ is converted into hydroxyl radicals, thereby improving the photocatalytic performance of the compound [49]. Besides, the degradation efficiency of MB with H₂O₂ (pH = 4: 56.95%; pH = 7: 76.77%; pH = 10: 95.69%) was higher than that without H₂O₂ (pH = 4: 46.65%; pH = 7: 54.34%; pH = 10: 61.20%) (Fig. 6). This is because when exposed to visible light, H₂O₂ decomposes into hydroxyl radicals, which interfere with the combination of hole and electron, thus enhance the photocatalytic performance [50].

Cycling experiments were performed to understand the repeatability of compound 1. As shown in Fig. 6, after 5 cycles, the degradation efficiencies of MB without and with H₂O₂ were decreased by 1.08% and 1.46%, respectively. The small decrease in degradation efficiency may be due to the little loss of sample in the recovery experiment.

It was found that the degradation speed of MB raised with time. As shown in Fig. 7, the relationship between ln(C_t/C₀) and time *t* is as follows:

$$\ln\left(\frac{C_t}{C_0}\right) = -kt \quad (3)$$

where C_{*t*} is the concentration of MB at time *t*, C₀ is the initial concentration of MB, and *k* is the apparent rate constant of MB for compound 1. It can be seen that the

concentration of MB has a first-order kinetic relationship with the time of visible light irradiation.

The photocatalytic degradation efficiency of compound 1 for MB in different traps was investigated. The addition of ethylenediaminetetraacetic acid (EDTA) which acts as holes scavenger. Isopropanol (IPA) and p-benzoquinone (PBQ) are used as hydroxyl radicals and superoxide radicals scavenger. It was found that when IPA or PBQ were added to the solution, there was only a small floating drop in the degradation efficiency. However, when EDTA was added, the degradation efficiency decreased by 33.4% (Fig. 8). Therefore, holes play a dominant role in the entire photocatalytic degradation process.

In order to better understand the photocatalytic mechanism of compound 1 under visible light. The energy band level of compound 1 was analyzed using the Mott–Schottky curve. As shown in Fig. 9, the positive slope of the Mott–Schottky curve for compound 1 indicates that the compound 1 is an *n*-type semiconductor. The flat band potential is -0.48 eV (vs. Ag/AgCl). In generally, the conduction band (CB) potential of *n*-type semiconductor is 0.1 V less than the flat band [51], so its conduction band potential is -0.58 eV. According to the formula $E_{\text{NHE}} = E_{\text{Ag/AgCl}} + 0.197 \text{ V}$ [52], the conduction band potential is -0.383 eV vs. the normal hydrogen electrode, which is lower than O₂/[•]O₂⁻ redox potential (-0.33 eV). This shows that compound 1 can reduce O₂ to [•]O₂⁻ by e⁻.

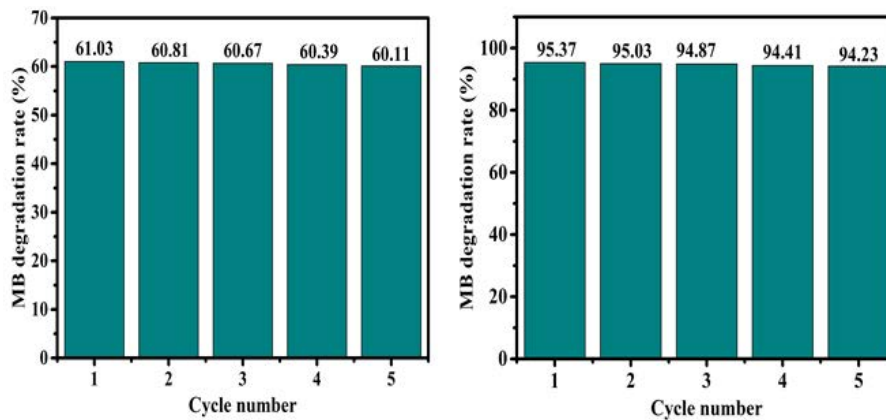


Fig. 6. Compound 1 recycling experiments in methylene blue photodegradation. Conditions: pH = 10, add compound 1 for (a); pH = 10, add compound 1 and H₂O₂ for (b).

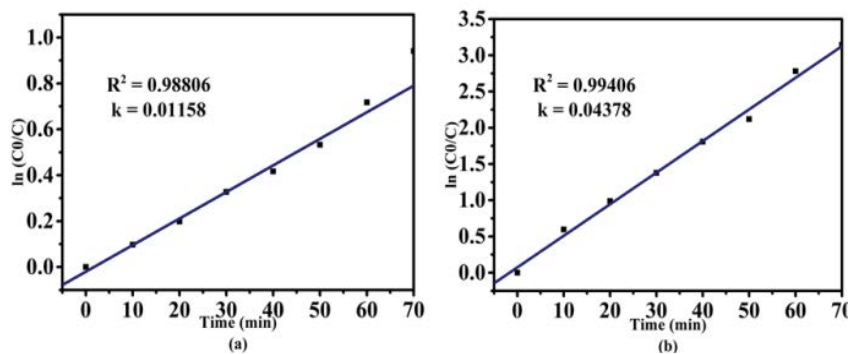


Fig. 7. Determination of kinetic parameters. Conditions: pH = 10, add compound 1 for (a); pH = 10, add compound 1 and H₂O₂ for (b).

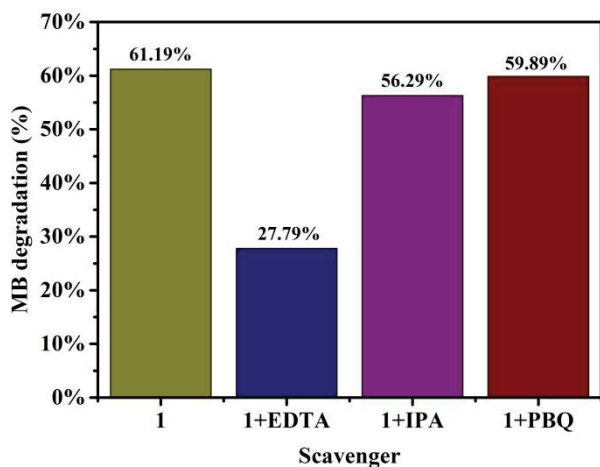


Fig. 8. Photocatalytic degradation efficiency of methylene blue by compound 1 in different scavengers.

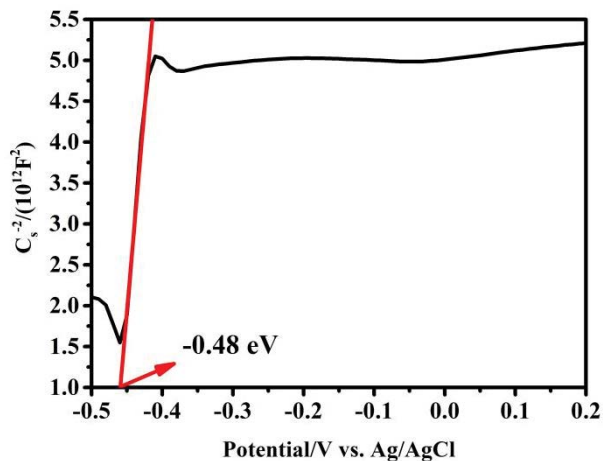


Fig. 9. Mott-Schottky plots of compound 1.

The valence band (VB) (vs. NHE) of compound 1 was estimated to be 2.197 eV based on the band gap energy (2.58 eV). The redox potential is higher than that of $\text{OH}^-/\cdot\text{OH}$ (1.99 eV), so the holes can oxidize OH^- to $\cdot\text{OH}$. According to the above speculation, the mechanism of photocatalytic degradation of MB by compound 1 under visible light may be as follows (Fig. 10):

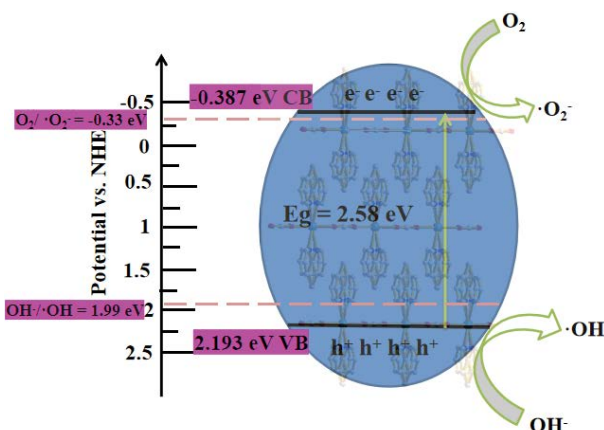
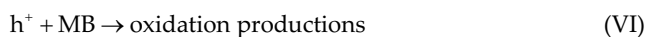
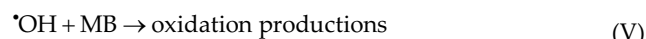
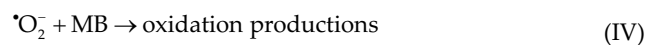


Fig. 10. Possible photocatalytic mechanism of compound 1 in visible light.



4. Conclusions

In summary, we reported the synthesis, structural characterization and photocatalysis property of a Pb(II) coordinated polymer $[\text{Pb}(\text{ox})(\text{phen})_2] \cdot 5\text{H}_2\text{O}$ 1. Based on the information obtained, several conclusions have been drawn: (i) through the analysis of UV-Vis diffuse reflectance and band gap calculation results, it is found that the catalyst has a photoresponse at visible light; (ii) compound 1 was found to be a potential visible photocatalyst based on the photocatalytic analysis. Photocatalytic degradation efficiency is as high as 95.69% under the irradiation of visible light and xenon lamp. Meanwhile, the photocatalytic results are consistent with first-order kinetics; (iii) it is worth noting that cycle effect of compound 1 is also excellent. After five cycles, the photocatalytic efficiency with and without H_2O_2 decreased by only 1.46% and 1.08%, respectively; (iv) it is also discussed which free radical plays the dominant role in the photocatalytic process. (v) Meanwhile, we speculated the possible reaction mechanism based on the Mott-Schottky curve. Therefore, the photocatalytic analysis suggests that compound 1 is a potential visible photocatalyst.

Acknowledgement

This research was supported by the Natural Science Foundation of Shandong Province (No. ZR2017PB006), the Open Foundation of State Key Laboratory of Inorganic Synthesis and Preparative Chemistry of Jilin University (No. 2023-20), the Natural Science Foundation of Ludong University (No. LY2014015), the Innovation Foundation for Students of Ludong University (No. 1d171040).

References

- [1] R. Toczyłowska-Mamińska, Limits and perspectives of pulp and paper industry wastewater treatment—a review, *Renewable Sustainable Energy Rev.*, 78 (2017) 764–772.
- [2] C. Thamaraiselvan, M. Noel, Membrane processes for dye wastewater treatment: recent progress in fouling control, *Crit. Rev. Env. Sci. Technol.*, 45 (2015) 1007–1040.

- [3] M. Muslim, A. Ali, I. Neogi, N. Dege, M. Shahid, M. Ahmad, Facile synthesis, topological study, and adsorption properties of a novel Co(II)-based coordination polymer for adsorptive removal of methylene blue and methyl orange dyes, *Polyhedron*, 210 (2021) 115519, doi: 10.1016/j.poly.2021.115519.
- [4] S. Rengaraj, X.Z. Li, Enhanced photocatalytic activity of TiO₂ by doping with Ag for degradation of 2,4,6-trichlorophenol in aqueous suspension, *J. Mol. Catal. A: Chem.*, 243 (2006) 60–67.
- [5] J.J. Xing, H. Liang, S.Q. Xu, C.J. Chuah, X.S. Luo, T.Y. Wang, J.L. Wang, G.B. Li, S.A. Snyder, Organic matter removal and membrane fouling mitigation during algae-rich surface water treatment by powdered activated carbon adsorption pretreatment: enhanced by UV and UV/chlorine oxidation, *Water Res.*, 159 (2019) 283–293.
- [6] S. Lin, Y. Zhao, J.K. Bediako, C.W. Cho, A.K. Sarkar, C.R. Lim, Y.S. Yun, Structure-controlled recovery of palladium(II) from acidic aqueous solution using metal-organic frameworks of MOF-802, UiO-66 and MOF-808, *Chem-Eur. J.*, 362 (2019) 280–286.
- [7] M.M. Chen, H.X. Li, J.P. Lang, Two coordination polymers and their silver(I)-doped species: synthesis, characterization, and high catalytic activity for the photodegradation of various organic pollutants in water, *Eur. J. Inorg. Chem.*, 2016 (2016) 2508–2515.
- [8] J. Jin, H.S. Li, W.F. Yan, Y.C. Wang, Q.A. Qiao, Q.J. Zhang, S.Y. Wu, Y.H. Lu, S.F. Ping, Z.Y. Jiang, Synthesis, structure and photocatalytic property of a novel Zn(II) coordination polymer based on *in-situ* synthesized pyridine-3,4-dicarboxyl-hydrazidate ligand, *Spectrochim. Acta, Part A*, 233 (2020) 118232, doi: 10.1016/j.saa.2020.118232.
- [9] J. Bedia, V. Muelas-Ramos, M. Penas-Garzon, A. Gomez-Aviles, J.J. Rodriguez, C. Belver, A review on the synthesis and characterization of metal organic frameworks for photocatalytic water purification, *Catalysts*, 9 (2019) 52, doi: 10.3390/catal9010052.
- [10] X. Li, B. Wang, Y.H. Cao, S. Zhao, H. Wang, X. Feng, J.W. Zhou, X.J. Ma, Water contaminant elimination based on metal-organic frameworks and perspective on their industrial applications, *ACS Sustainable Chem. Eng.*, 7 (2019) 4548–4563.
- [11] Y.J. Huang, G. Du, J. Zhang, Syntheses, structural characterization and properties of nickel(II) coordination polymer with 1,3,5-tris(1H-pyrazol-3-yl)benzene and succinic acid, *J. Chem. Crystallogr.*, 50 (2020) 28–34.
- [12] H. Tong, S. Ouyang, Y.B. Bi, N. Umezawa, M. Oshikiri, J.H. Ye, Nano-photocatalytic materials: possibilities and challenges, *Adv. Mater.*, 24 (2012) 229–251.
- [13] Z.Q. Liu, A.M. Andrade, S. Grewal, A.J. Nelson, K. Thongrivorong, H.S. Kang, H.Y. Li, Z. Nasef, G. Diaz, M.H. Lee, Trace amount of ceria incorporation by atomic layer deposition in Co/CoOx-embedded N-doped carbon for efficient bifunctional oxygen electrocatalysis: demonstration and quasi-operando observations, *Int. J. Hydrogen Energy*, 46 (2021) 38258–38269.
- [14] R. Sen, R. Halder, D. Ghoshal, Three mixed ligand coordination polymers: syntheses, characterization and detailed study of the structural transformations, *Polyhedron*, 183 (2020) 114534, doi: 10.1016/j.poly.2020.114534.
- [15] A. Halder, B. Bhattacharya, F. Haque, D. Ghoshal, Structural diversity in six mixed ligand Zn(II) metal-organic frameworks constructed by rigid and flexible dicarboxylates and different N,N' donor ligands, *Cryst. Growth Des.*, 17 (2017) 6613–6624.
- [16] J. Liu, J. Zheng, D. Barpaga, S. Sabale, B. Arey, M.A. Derewinski, B.P. McGrail, R.K. Motkuri, A tunable bimetallic MOF-74 for adsorption chiller applications, *Eur. J. Inorg. Chem.*, 2018 (2018) 885–889.
- [17] J. Jin, Y.C. Wang, W.F. Yan, C. Wang, W.L. Wang, Y.Z. Niu, B.Q. Yuan, H. Xu, H.S. Li, Q.J. Zhang, Synthesis and properties of Mg²⁺ and Sr²⁺ coordination compounds based on *in situ* synthesized pyromellitidihydrazidate ligand, *J. Mol. Struct.*, 1204 (2020) 127560, doi: 10.1016/j.molstruc.2019.127560.
- [18] R.B. Lin, T.Y. Li, H.L. Zhou, C.T. He, J.P. Zhang, X.M. Chen, Tuning fluorocarbon adsorption in new isorecticular porous coordination frameworks for heat transformation applications, *Chem. Sci.*, 6 (2015) 2516–2521.
- [19] Z.J. Lin, J. Lü, M.C. Hong, R. Cao, Metal-organic frameworks based on flexible ligands (FL-MOFs): structures and applications, *Chem. Soc. Rev.*, 43 (2014) 5867–5895.
- [20] T. Baran, A. Mentes, Highly efficient Suzuki cross-coupling reaction of biomaterial supported catalyst derived from glyoxal and chitosan, *J. Organomet. Chem.*, 803 (2016) 30–38.
- [21] X. Zhang, X. Luo, N.X. Zhang, J. Wu, Y.Q. Huang, A highly selective and sensitive Zn(II) coordination polymer luminescent sensor for Al³⁺ and NACs in the aqueous phase, *Inorg. Chem. Front.*, 4 (2017) 1888–1894.
- [22] Y.C. Guo, Z.Y. Jiang, Y.C. Wang, J. Jin, W.F. Yan, Z.X. Zhao, Y.M. Ma, L.Y. Yan, Z.Q. Jiang, Q.A. Qiao, Synthesis, structure and photocatalytic property of the 1D oxalate-bridged coordination polymer of manganese(II), *J. Mol. Struct.*, 1251 (2022) 131961, doi: 10.1016/j.molstruc.2021.131961.
- [23] H.L. Zhu, D.X. Liu, D.T. Zou, J.Y. Zhang, The photo-, electro- and photoelectro-catalytic properties and application prospects of porous coordinate polymers, *J. Mater. Chem. A*, 6 (2018) 6130–6154.
- [24] H.C. Zhou, J.R. Long, O.M. Yaghi, Introduction to metal-organic frameworks, *Chem. Rev.*, 112 (2012) 673–674.
- [25] X.J. Zheng, L.C. Li, S. Gao, L.P. Jin, Hydrothermal syntheses, structures and magnetic properties of two transition metal coordination polymers with a square grid framework, *Polyhedron*, 23 (2004) 1257–1262.
- [26] S.L. Cai, L. Lu, W.P. Wu, J. Wang, Y.C. Sun, A.Q. Ma, A. Singh, A. Kumar, A new mixed ligand based Cd(II) 2D coordination polymer with functional sites: photoluminescence and photocatalytic properties, *Inorg. Chim. Acta*, 484 (2019) 291–296.
- [27] S. Phengthaisong, A. Cheansirisomboon, J. Boonmak, S. Youngme, The crystal structure and photocatalytic properties of a cobalt(II) coordination polymer based on 4,4'-oxy(bis)benzoic acid, *Inorg. Chem. Commun.*, 88 (2018) 21–24.
- [28] Z.T. Yu, Z.L. Liao, Y.S. Jiang, G.H. Li, G.D. Li, J.S. Chen, Construction of a microporous inorganic-organic hybrid compound with uranyl units, *Chem. Commun.*, 16 (2004) 1814–1815.
- [29] N.N. Chen, J.L. Ni, J. Wang, A new two-dimensional Co(II) coordination polymer based on bis[4-(2-methyl-1H-imidazol-1-yl)phenyl] ether and biphenyl-4,4'-diyl dicarboxylic acid: synthesis, crystal structure and photocatalytic degradation activity, *Acta Crystallogr., Sect. C: Cryst. Struct. Commun.*, 74 (2018) 1123–1127.
- [30] T.S. Xue, W.W. Cheng, Z.L. Chen, W. Kong, J. Zhang, A novel three-dimensional zinc(II) coordination polymer based on 3,3'-[1,3-phenylenebis(methylene)]bis(oxy) dibenzoic acid and 1,4-bis(pyridin-4-yl)benzene: synthesis, crystal structure and photocatalytic properties, *Acta Crystallogr., Sect. C: Cryst. Struct. Commun.*, 76 (2020) 453–358.
- [31] J. Jin, H. Chen, X. Zhang, Y.C. Wang, Z.J. Zhang, Q.F. Yang, C. Lin, J.R. Li, Q.J. Zhang, Synthesis, structural characterization and photoluminescence property of two Zn²⁺/In³⁺-4,4'-oxydiphthalhydrazidate complexes, *Inorg. Chim. Acta*, 482 (2018) 1–7.
- [32] J. Jin, W.F. Yan, Q.F. Yang, X.T. Yu, L.X. Sun, J.Q. Xu, Z.A. Chen, C.Z. Li, New oxalate-propagated layered Mn²⁺/Fe²⁺-4,4-sulfoylidiphthalhydrazidate coordination polymers, *J. Mol. Struct.*, 1127 (2017) 303–308.
- [33] H. Dai, S. Xu, J. Chen, X. Miao, J. Zhu, Oxalate enhanced degradation of Orange II in heterogeneous UV-Fenton system catalyzed by Fe₃O₄@γ-Fe₂O₃ composite, *Chemosphere*, 199 (2018) 147–153.
- [34] R. Dridi, S.N. Cherni, F. Fettar, N. Chniba-Boudjada, M.F. Zid, A novel oxalate-based three dimensional polymorphs supramolecular compounds: synthesis, spectroscopic characterization, magnetic and photocatalytic properties, *J. Mol. Struct.*, 1205 (2020) 127573, doi: 10.1016/j.molstruc.2019.127573.
- [35] J. Jin, W.F. Yan, X.Y. Yu, Q.F. Yang, B. Liu, J.Q. Xu, S.M. Gao, C.Z. Li, C. Lin, New 4-carboxylphthalhydrazidate-bridged Mn²⁺/In³⁺ coordination polymers, *J. Mol. Struct.*, 1134 (2017) 728–733.

- [36] M.M. El-bendary, T. Rüffer, M.N. Arshad, A.M. Asiri, Synthesis and structure characterization of Pt(IV) and Cd(II) 1,10-phenanthroline complexes: fluorescence, antitumor and photocatalytic property, *J. Mol. Struct.*, 1192 (2019) 230–240.
- [37] L. Lu, J. Wang, C.Y. Shi, X.D. Jiang, Y.C. Sun, W.P. Wu, W.X. Hu, Four new coordination complexes prepared for the degradation of methyl violent dye based on flexible dicarboxylate and different N-donor coligands, *J. Mol. Struct.*, 1225 (2021) 129181, doi: 10.1016/j.molstruc.2020.129181.
- [38] X.Y. Li, L. Gao, Y.Q. Niu, C.B. Liu, G.B. Che, Y.S. Yan, Q.F. Guan, Pb(II) coordination polymer based on mixed ligands: syntheses, structures, photoluminescence, and photocatalysis, *J. Inorg. Organomet. Polym.*, 25 (2014) 886–891.
- [39] L.H. Zhu, M.H. Zeng, B.H. Ye, X.M. Chen, Hydrothermal synthesis and crystal structure of a new oxalato-bridged lead (II) polymer: $\{[\text{Pb}(\text{phen})_2(\text{ox})] \cdot 5\text{H}_2\text{O}\}_n$ (phen = 1,10-phenanthroline, ox = oxalate), *Z. Anorg. Allg. Chem.*, 630 (2004) 952–955.
- [40] G.L. Li, W.D. Yin, Q.L. Liu, X.R. Gong, Y.J. Zhao, G.Z. Liu, N-donor-induced two Co(II) coordination polymers derived from the flexible citraconic acid as photocatalysts for the decomposition of organic dyes, *Z. Anorg. Allg. Chem.*, 648 (2022) e202100037, doi: 10.1002/zaac.202100037.
- [41] S.E.D.H. Etaiw, H. Marie, 3D-Supramolecular coordination polymer nanoparticles based on Cd(II) and mixed ligands: single crystal X-ray structure, luminescence and photocatalytic properties, *J. Inorg. Organomet. Polym.*, 28 (2018) 508–518.
- [42] S.E.D.H. Etaiw, H. Marie, Ultrasonic synthesis of 1D-Zn(II) and La(III) supramolecular coordination polymers nanoparticles, fluorescence, sensing and photocatalytic property, *J. Photochem. Photobiol., A*, 364 (2018) 478–491.
- [43] L. Qin, H.Z. Chen, J. Lei, Y.Q. Wang, T.Q. Ye, H.Z. Zheng, Photodegradation of some organic dyes over two metal-organic frameworks with especially high efficiency for safranin T, *Cryst. Growth Des.*, 17 (2017) 1293–1298.
- [44] Y.H. Zhao, Z.Y. Zhang, T.P. Cao, L. Wang, Y. Fan, T. Wan, J. Jia, Construction of luminescent coordination polymers based on 5-(1-(carboxymethyl)-pyrazol-3-yl)isophthalic ligand for sensing Cu^{2+} and acetone, *Polyhedron*, 177 (2020) 114314, doi: 10.1016/j.poly.2019.114314.
- [45] A. Morsali, A.R. Mahjoub, H.R. Bijanzadeh, Crystal structure of nitrate-O,O'-bis(1,10-phenanthroline) nitritolead(II), $\text{Pb}(\text{phen})_2(\text{NO}_3)_2(\text{NO}_2)_{0.5}$, *Z. Kristallogr. - New Cryst. Struct.*, 218 (2003) 189–190.
- [46] W.H. Mahmoud, G.G. Mohamed, S.Y.A. Sabrine, Spectroscopic characterization, thermal, antimicrobial and molecular docking studies on nano-size mixed ligand complexes based on sudan III azodye and 1,10-phenanthroline, *J. Therm. Anal. Calorim.*, 130 (2017) 2167–2184.
- [47] J. Tauc, Absorption edge and internal electric fields in amorphous semiconductors, *Mater. Res. Bull.*, 5 (1970) 721–729.
- [48] R.H. Hou, P. Han, Q. Liu, G.R. Xu, S.J. Xu, T. Chen, A new Zn(II)-coordination polymer based on m-terphenyl pentacarboxylic acid ligand for photocatalytic methylene blue degradation and protective effect against Alzheimer's disease by reducing the inflammatory response and oxidative stress in the nerve cells, *Arabian J. Chem.*, 13 (2020) 5171–5180.
- [49] S. Sakthivel, B. Neppolian, M.V. Shankar, B. Arabindoo, M. Palanichamy, V. Murugesan, Solar photocatalytic degradation of azo dye: comparison of photocatalytic efficiency of ZnO and TiO_2 , *Sol. Energy Mater. Sol. Cells*, 77 (2003) 65–82.
- [50] J.J. Wang, L.B. Wang, Z. Cao, E.L. Yue, L. Tang, X. Wang, X.Y. Hou, Y.Q. Zhang, Four coordination polymers based on 5-(3,5-dicarboxybenzyloxy) isophthalic acid: synthesis, structures, photocatalytic properties, fluorescence sensing and magnetic properties, *J. Solid State Chem*, 302 (2021) 122379, doi: 10.1016/j.jssc.2021.122379.
- [51] Y.W. Gao, S.M. Li, Y.X. Li, L.Y. Yao, H. Zhang, Accelerated photocatalytic degradation of organic pollutant over metal-organic framework MIL-53(Fe) under visible LED light mediated by persulfate, *Appl. Catal., B*, 202 (2017) 165–174.
- [52] M. Gopannagari, D.P. Kumar, H. Park, E.H. Kim, P. Bhavani, D.A. Reddy, T.K. Kim, Influence of surface-functionalized multi-walled carbon nanotubes on CdS nanohybrids for effective photocatalytic hydrogen production, *Appl. Catal., B*, 236 (2018) 294–303.

Supporting information

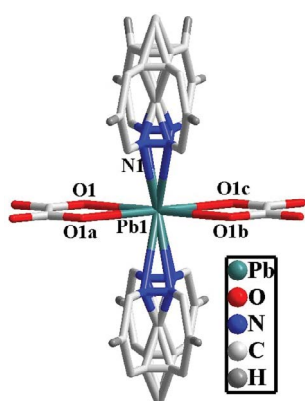


Fig. S1. Coordination environment of Pb^{2+} center in compound 1 (symmetric code a: $-x+1, -y+1, -z+1$; b: $x, y, -z+1$; c: $-x+1, -y+1, z$).

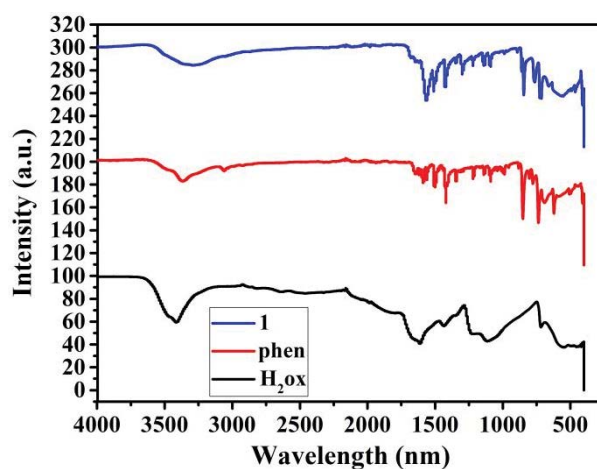


Fig. S2. Infrared spectrogram of compound 1, phen and H_2ox .

Datablock:

1

| | | | |
|---|--|--|--------------------|
| Bond precision: | C-C = 0.0180 Å | | Wavelength=1.54184 |
| Cell: | $a = 19.3535(10)$ | $b = 6.8144(4)$ | $c = 9.6731(10)$ |
| | $\alpha = 90$ | $\beta = 90$ | $\gamma = 90$ |
| Temperature: | 293 K | | |
| Volume | Calculated | Reported | |
| | 1,275.71(17) | 1,275.71(17) | |
| Space group | C_{mmm} | C_{mmm} | |
| Hall group | -C 2 2 | -C 2 2 | |
| Moiety formula | $\text{C}_{26}\text{H}_8\text{N}_4\text{O}_4\text{Pb}$ [+ solvent] | $\text{C}_{26}\text{H}_8\text{N}_4\text{O}_4\text{Pb}$ | |
| Sum formula | $\text{C}_{26}\text{H}_8\text{N}_4\text{O}_4\text{Pb}$ [+ solvent] | $\text{C}_{26}\text{H}_8\text{N}_4\text{O}_4\text{Pb}$ | |
| Mr | 647.56 | 647.55 | |
| D_x , g/cm ³ | 1.686 | 1.686 | |
| Z | 2 | 2 | |
| Mu (mm ⁻¹) | 13.177 | 13.177 | |
| F000 | 612.0 | 612.0 | |
| F000' | 605.50 | | |
| h, k, l_{max} | 23, 8, 11 | 23, 8, 11 | |
| N_{ref} | 743 | 735 | |
| $T_{\text{min}}, T_{\text{max}}$ | | 0.795, 1.000 | |
| T_{min}' | | | |
| Correction method = # Reported T limits: $T_{\text{min}} = 0.795$ $T_{\text{max}} = 1.000$ AbsCorr = MULTI-SCAN | | | |
| Data completeness = 0.989 | | Theta(max) = 71.359 | |
| $R(\text{reflections}) = 0.0448(727)$ | | $wR_2(\text{reflections}) = 0.1063(735)$ | |
| $S = 1.081$ | | $N_{\text{par}} = 71$ | |

The following ALERTS were generated. Each ALERT has the format

test-name_ALERT_alert-type_alert-level.

Click on the hyperlinks for more details of the test.

Alert level B

PLAT241_ALERT_2_B High 'MainMol' Ueq as Compared to Neighbors of O1 Check

Alert level C

PLAT053_ALERT_1_C Minimum Crystal Dimension Missing (or Error) ... Please Check
 PLAT054_ALERT_1_C Medium Crystal Dimension Missing (or Error) ... Please Check
 PLAT055_ALERT_1_C Maximum Crystal Dimension Missing (or Error) ... Please Check
 PLAT242_ALERT_2_C Low 'MainMol' Ueq as Compared to Neighbors of ... Pb1 Check
 PLAT342_ALERT_3_C Low Bond Precision on C–C Bonds ... 0.018 Ang.
 PLAT975_ALERT_2_C Check Calcd Resid. Dens. 0.82Ang From C6 0.68 eA-3
 And 4 other PLAT975 Alerts
 More ...
 PLAT976_ALERT_2_C Check Calcd Resid. Dens. 0.89Ang From O1 -0.49 eA-3

Alert level G

PLAT004_ALERT_5_G Polymeric Structure Found with Maximum Dimension 1 Info
 PLAT199_ALERT_1_G Reported _cell_measurement_temperature ... (K) 293 Check
 PLAT200_ALERT_1_G Reported _diffrn_ambient_temperature ... (K) 293 Check
 PLAT300_ALERT_4_G Atom Site Occupancy of N1 Constrained at 0.5 Check
 And 6 other PLAT300 Alerts
 More ...
 PLAT301_ALERT_3_G Main Residue Disorder ... (Resd 1) 52% Note
 PLAT605_ALERT_4_G Largest Solvent Accessible VOID in the Structure 104 A**3
 PLAT789_ALERT_4_G Atoms with Negative _atom_site_disorder_group # 7
 Check
 PLAT811_ALERT_5_G No ADDSYM Analysis: Too Many Excluded Atoms ...! Info
 PLAT869_ALERT_4_G ALERTS Related to the Use of SQUEEZE Suppressed ! Info
 PLAT912_ALERT_4_G Missing # of FCF Reflections Above STh/L = 0.600 8 Note
 PLAT941_ALERT_3_G Average HKL Measurement Multiplicity ... 2.0 Low
 PLAT961_ALERT_5_G Dataset Contains no Negative Intensities ... Please Check
 PLAT978_ALERT_2_G Number C–C Bonds with Positive Residual Density 0 Info